



ELSEVIER

Available online at www.sciencedirect.com

SCIENCE @ DIRECT®

Global and Planetary Change 36 (2003) 219–235

GLOBAL AND PLANETARY
CHANGE

www.elsevier.com/locate/gloplacha

The response of the African summer monsoon to remote and local forcing due to precession and obliquity

E. Tuenter^{a,b,*}, S.L. Weber^a, F.J. Hilgen^b, L.J. Lourens^b

^aRoyal Netherlands Meteorological Institute (KNMI), P.O. Box 201, 3730 AE De Bilt, The Netherlands

^bDepartment of Geology, Faculty of Earth Sciences, Utrecht University, Budapestlaan 4, 3584 CD Utrecht, The Netherlands

Received 28 February 2002; accepted 4 September 2002

Abstract

In this paper, we examine the orbital signal in Earth's climate with a coupled model of intermediate complexity (ECBilt). The orbital influence on climate is studied by isolating the obliquity and precession signal in several time-slice experiments. Focus is on monsoonal systems with emphasis on the African summer monsoon. The model shows that both the precession and the obliquity signal in the African summer monsoon consists of an intensified precipitation maximum and further northward extension during minimum precession and maximum obliquity than during maximum precession and minimum obliquity. In contrast to obliquity, precession also influences the seasonal timing of the occurrence of the maximum precipitation. The response of the African monsoon to orbital-induced insolation forcing can be divided into a response to insolation forcing at high northern latitudes and a response to insolation forcing at low latitudes, whereby the former dominates. The results also indicate that the amplitude of the precipitation response to obliquity depends on precession, while the precipitation response to precession is independent of obliquity. Our model experiments provide an explanation for the precession and obliquity signals in sedimentary records of the Mediterranean (e.g., Lourens et al. [Paleoceanography 11 (1996) 391, Nature 409 (2001) 1029]), through monsoon-induced variations in Nile river outflow and northern Africa aridity.

© 2003 Elsevier Science B.V. All rights reserved.

Keywords: precession; obliquity; African summer monsoon; climate modeling

1. Introduction

The deposition of successive sapropels (organic-rich black layers) in the eastern Mediterranean Sea has been related to astronomical forcing of the climate. Individual sapropels are correlated with strong Northern Hemisphere (NH) summer insolation which is

associated with minimum peaks in the orbital precession index (Rossignol-Strick, 1983; Hilgen, 1991). The orbital precession index is defined as $e \sin \tilde{\omega}$ where e is the eccentricity of the Earth orbit and $\tilde{\omega}$ is the longitude of the perihelion. Rossignol-Strick (1983) first showed that a sapropel is formed every time that the boreal summer insolation produces an African monsoon index above a certain threshold (i.e., a strong African monsoon). A higher insolation leads to an enhanced temperature contrast between land and ocean which leads, in its turn, to a larger land–ocean pressure difference and thus to an intensified low-

* Corresponding author. Royal Netherlands Meteorological Institute (KNMI), P.O. Box 201, 3730 AE De Bilt, The Netherlands. Tel.: +31-30-2206769; fax: +31-30-2202570.

E-mail address: tuentere@knmi.nl (E. Tuenter).

level monsoonal flow. The heavy discharge of the river Nile which is associated with strong monsoons, could result in the forming of Mediterranean sapropels.

Tropical insolation is precession dominated. Besides the sapropels, this is also reflected in other paleoclimatic data showing strong precessional components in the boreal summer monsoons. Examples are records of abundance of planktic foraminifera from the Arabian Sea indicating coastal upwelling strength which is related to the strength of the southwest Indian monsoon surface wind fields (Prell, 1984), or the occurrence of eolian freshwater diatoms in equatorial Atlantic deep-sea sediments, indicating periods of aridity in tropical Africa (Pokras and Mix, 1987).

However, Lourens et al. (1996, 2001) found alternating thick/thin sapropels in the Mediterranean Sea reflecting a pronounced obliquity component, whereby thick (thin) sapropels correspond to obliquity maxima (minima). This suggests that apart from a precessional component, also an obliquity signal is present in the strength of the African monsoon.

Several model studies found clear orbital signals in the monsoonal systems. A large number of these studies simulate a combined precession and obliquity signal, where precession dominates obliquity effects. For example, model simulations show that on the NH the summer monsoon circulation strengthened after the Last Glacial Maximum (~ 18,000 years Before Present (18 ka BP)), attaining its maximum in the early Holocene (~ 9 ka BP) and then weakening to its modern-day strength (Kutzbach and Street-Perrott, 1985). This signal coincides with the NH summer insolation which also increased after 18 ka BP with a maximum at 9 ka BP. Other studies confirmed the enhanced monsoonal strength at 9 ka BP (Kutzbach, 1981; Kutzbach and Otto-Bliesner, 1982). Just a few studies separate the precession and obliquity signal and most of these studies use an Energy Balance Model (EBM) (Suarez and Held, 1979; Harvey, 1989; Short et al., 1991). However, these studies only give an indirect indication of obliquity and precession signals in the monsoon by signals in the tropical temperature (Short et al., 1991).

Both a precession and an obliquity signal in the African monsoon has been found using several generic radiation pattern with an Atmospheric General

Circulation Model (AGCM) in permanent July mode (Prell and Kutzbach, 1987), a result which seems to be confirmed by the sedimentary analysis of Lourens et al. (1996, 2001). Remarkably, the largest insolation amplitude that is associated with obliquity is found at high latitudes.

Concerning the response of the monsoons to obliquity and precession, a number of problems remain: What is the physical mechanism with which the obliquity signal can manifest itself in the African monsoon strength? Or, alternatively, are changes of monsoon intensity caused by solar radiation at high latitudes, at low latitudes or at a combination of latitudes? Do orbital variations influence the spatial pattern and timing of the monsoons? Finally, does the sensitivity of the monsoons to precession and obliquity depend on the background climatic state, or, alternatively, the prevailing orbital configuration?

To address these questions, we examined both the obliquity and precession signal in the climate with focus on the African summer monsoon using a model of intermediate complexity (ECBilt). As opposed to Prell and Kutzbach (1987), we examine the orbital influences on the seasonal cycle of the African monsoon and we use a more extensive set of orbital parameters. Furthermore, we distinguish the orbital influences originating from higher latitudes and from lower latitudes.

The model and experimental set-up used for the simulations are described in Section 2. Section 3 gives some global results concerning orbital influences on temperature, precipitation and circulation, while in Section 4 the African monsoon will be discussed. Section 5 presents additional experiments providing some insights into the mechanisms of the African monsoon. The study is concluded and discussed in Section 6.

2. The model and experimental set-up

ECBilt (Opsteegh et al., 1998) is a global fully coupled atmosphere/ocean/sea-ice climate model of intermediate complexity. The horizontal resolution is about 500 km in mid-latitudes for both the ocean and the atmosphere (spectral T21 for the atmosphere). The vertical resolution is three layers for the atmosphere and 12 layers for the ocean. The time step for the

atmosphere is 4 h and for the ocean 1 day. No flux corrections are used. The dynamics of the atmosphere is based on quasi-geostrophic equations but ageostrophic components are included as a (diagnostically computed) time- and spatially varying potential vorticity forcing. Due to the ageostrophic forcing the Hadley circulation is simulated qualitatively correct but it is still too weak. The land surface scheme consists of a bucket model for the soil moisture and a thermodynamic snow model. The ocean has a flat bottom and the dynamics are based on primitive equations. Finally, the sea-ice model is a thermodynamic model with no ice dynamics.

The model is very suitable for performing several (sensitivity) simulations and for long paleoclimate simulations due to its computational efficiency (Van der Schrier et al., 2002; Weber and Oerlemans, 2003). Compared to observations, the present-day mean climate is simulated reasonably well. In particular, both the strength and spatial pattern of the mean annual cycle of the African summer monsoon precipitation are simulated quite well compared to the NCEP/NCAR reanalysis (Kistler et al., 2001). For example, the precipitation averaged over the monsoon region (15°W–30°E, 0–20°N) shows a maximum in August in ECBilt (~ 5.4 mm/day) and in the NCEP/NCAR reanalysis (~ 4.8 mm/day). The annual variability is underestimated in the model which is mainly due to the quasi-geostrophic equations. However, in the present study, only the mean pattern and strength of the monsoon are studied. Weber (2001) compared a simulation for 6 ka BP performed by ECBilt with experiments performed by models within the Paleo Modeling Intercomparison Project (PMIP). This comparison puts ECBilt in the middle (for the African monsoon) to lower (for the Asian monsoon) range of the PMIP results concerning the sensitivity of monsoonal precipitation to insolation changes (Joussaume et al., 1999; Braconnot et al., 2002b).

In order to investigate the obliquity and the precession signal in the climate, six sensitivity experiments with different orbital configurations have been performed:

1. Minimum precession with minimum obliquity or tilt (P – T –),
2. Maximum precession with minimum obliquity (P + T –),
3. Minimum precession with maximum obliquity (P – T+),
4. Maximum precession with maximum obliquity (P + T+),
5. Circular Earth orbit (i.e., eccentricity=0) with minimum obliquity (P0T –),
6. Circular Earth orbit with maximum obliquity (P0T+).

We took extreme values of the orbital parameters occurring in the last 1,000,000 years (1 Ma). The values of these orbital parameters and the corresponding insolation were calculated by the method of Berger (1978), see Table 1 for a survey. Extreme values of the precession index $esin\tilde{\omega}$ rather than extreme values of $\tilde{\omega}$ are considered, because precession is modulated by eccentricity. Therefore, it is necessary to include eccentricity. We use the terms “minimum” and “maximum” precession referring to the minimum and maximum values of $esin\tilde{\omega}$, respectively. Note from Table 1 that the eccentricities of the maximum and minimum precession are not equal. However, the difference is very small, which consequently also applies to the difference in global mean annual insolation.

For each experiment, the model was run for a period of 500 years, with present-day conditions as initial state. The first 400 years of the simulation were regarded as a spin-up period. After 400 years, the upper and mid-layers of the ocean were in equilibrium. The deep layers still showed trends. These

Table 1
Orbital parameters used for the six sensitivity experiments

Orbital parameter	Tilt (deg)	$esin\tilde{\omega}$	e	$\tilde{\omega}$ (deg)	Occurrence (ka BP)
P+		0.058	0.058	86.5	970
P–		–0.055	0.056	264.0	959
T+	24.45				213
T–	22.08				232
P0		0.0	0.0	–	–

P+, P–, T+ and T– are maximum precession, minimum precession, maximum tilt and minimum tilt, respectively. A precession maximum (minimum) means winter (summer) solstice in perihelion. The tilt is defined as the angle between the ecliptic and the equator, e is the eccentricity of the orbit of the Earth and $\tilde{\omega}$ is the angle between the vernal equinox and perihelion (measured clockwise). P0 is the simulation with a circular Earth orbit. The time of occurrence is given in 1000 years Before Present.

deep-ocean trends are comparable in amplitude to those found in the control run. The only forcing is the insolation changes due to the orbital parameters which were kept constant during the simulations. All other boundary conditions (like orography, concentration of trace gases and surface characteristics (e.g., albedo, roughness)) were kept to present-day values.

We will primarily consider four ‘basic’ experiments: the precession signal with a minimum obliquity and the obliquity signal with a circular Earth orbit. The latter is used to examine the obliquity signal because during a circular Earth orbit there is no influence of precession (i.e., $e \sin \tilde{\omega} = 0$ for each $\tilde{\omega}$). The other experiments will be discussed when there are significant differences with the basic precession and obliquity experiments.

3. Global results

In this section, we present the global differences between minimum and maximum precession, and minimum and maximum obliquities in December–January–February (DJF) and June–July–August (JJA). The results are averaged over the last 100 years of the 500-year simulations. A local, two-sided Student’s t-test is used to determine statistical significance.

Fig. 1A shows the incoming insolation differences at the top of the atmosphere caused by precession changes. In boreal spring and summer the minimum precession insolation is much larger than the maximum precession insolation, with the largest differences on the NH. This is caused by the summer solstice in perihelion and by the high eccentricity. In boreal winter the maximum precession insolation is larger with the largest differences on the Southern Hemisphere (SH). This means that precession enhances the seasonality on the NH and weakens it on the SH.

Insolation changes caused by obliquity show a very clear asymmetrical pattern with respect to the equator with more (less) boreal summer (winter) insolation during maximum obliquity on the NH (Fig. 1B). This figure also shows that the insolation at low latitudes is barely influenced by obliquity and that obliquity enhances the contrast between the hemispheres during summer and winter.

Fig. 2A–D shows that in DJF and JJA, the obliquity- and precession-induced differences of the

surface air temperature (SAT) are largest over the landmasses and smallest over the oceans. The latter is caused by the damping effects of the oceans due to their large thermal inertia. In general, the SAT-response is proportional to the forcing. The positive precession and obliquity signal over the Labrador Sea in DJF is related to sea-ice effects. The relatively small SAT-response over the tropical regions in JJA (even negative for obliquity, Fig. 2D) is related to the monsoon response, which will be discussed below.

Changes in SAT, precipitation and circulation due to changes in precession are similar whether obliquity is set to minimum values (i.e., P – T – and P + T –) or to maximum values (P – T + and P + T +). This also applies to the obliquity signal when precession is set to maximum values (i.e., P + T + and P + T –) or to a circular Earth orbit (i.e., P0T + and P0T –). However, over the NH landmasses in JJA the SAT-response to the obliquity signal during minimum precession is much larger (not shown), although the insolation differences are very similar compared to the other obliquity experiments. The pattern of the obliquity-induced SAT-differences during minimum precession is similar to the pattern shown in Fig. 2D but the maximum differences are about 4–5°C over central Asia and over Europe and 3°C over North America. This can be explained by strong evaporation in late spring and early summer due to the relatively high temperatures during minimum precession, causing very low soil moisture in summer. Therefore, the additional insolation due to a maximum obliquity only heats the atmosphere, rather than both increasing the evaporation and heating the atmosphere.

Both precession and obliquity results show that the temperature response to insolation changes is linear in ECBilt, except for certain regions like the Labrador Sea and the tropics. Apart from these regions, the temperature response of ECBilt is consistent with the response of an EBM using similar orbital parameters (Short et al., 1991).

In JJA, the precession signal in the precipitation shows a much stronger Asian and African monsoon during minimum precession (Fig. 3A). Also over eastern North America and over northern South America, the precipitation is stronger during minimum precession. The increased precipitation over the monsoon regions is at the expense of the precipitation over the oceans. The obliquity signal (Fig. 3B) con-

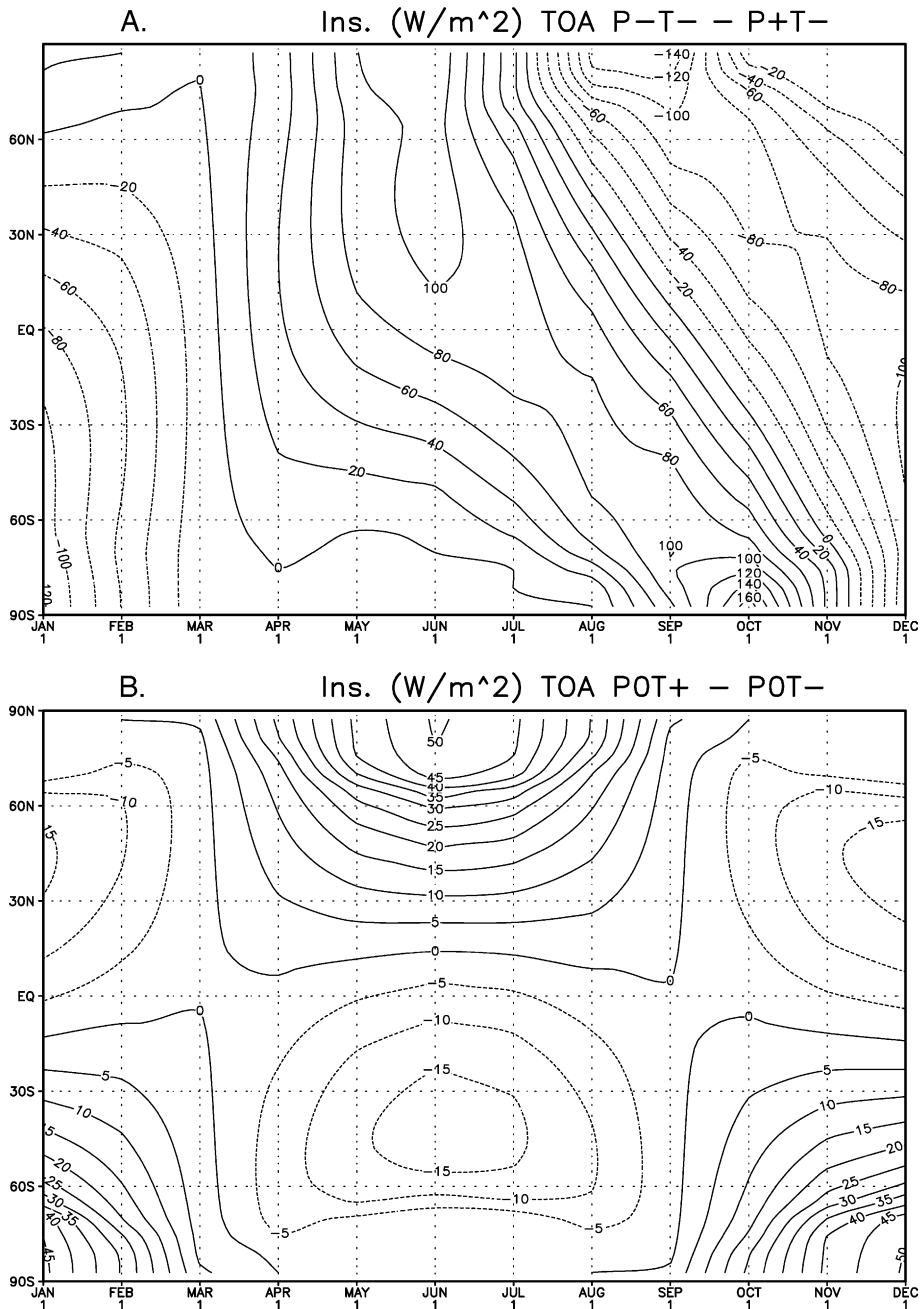


Fig. 1. Monthly incoming insolation differences in W/m^2 at the top of the atmosphere. See Table 1 for an explanation of the symbols. (A) Minimum precession minus maximum precession. Contour interval is $20 W/m^2$. (B) Maximum obliquity minus minimum obliquity. Contour interval is $5 W/m^2$.

sists of an intensified African and Asian monsoon and stronger precipitation over eastern North America during maximum obliquity, while over northern South

America the response is negative. Heating (cooling) of land relative to the ocean apparently causes stronger (weaker) monsoonal circulation and associated pre-

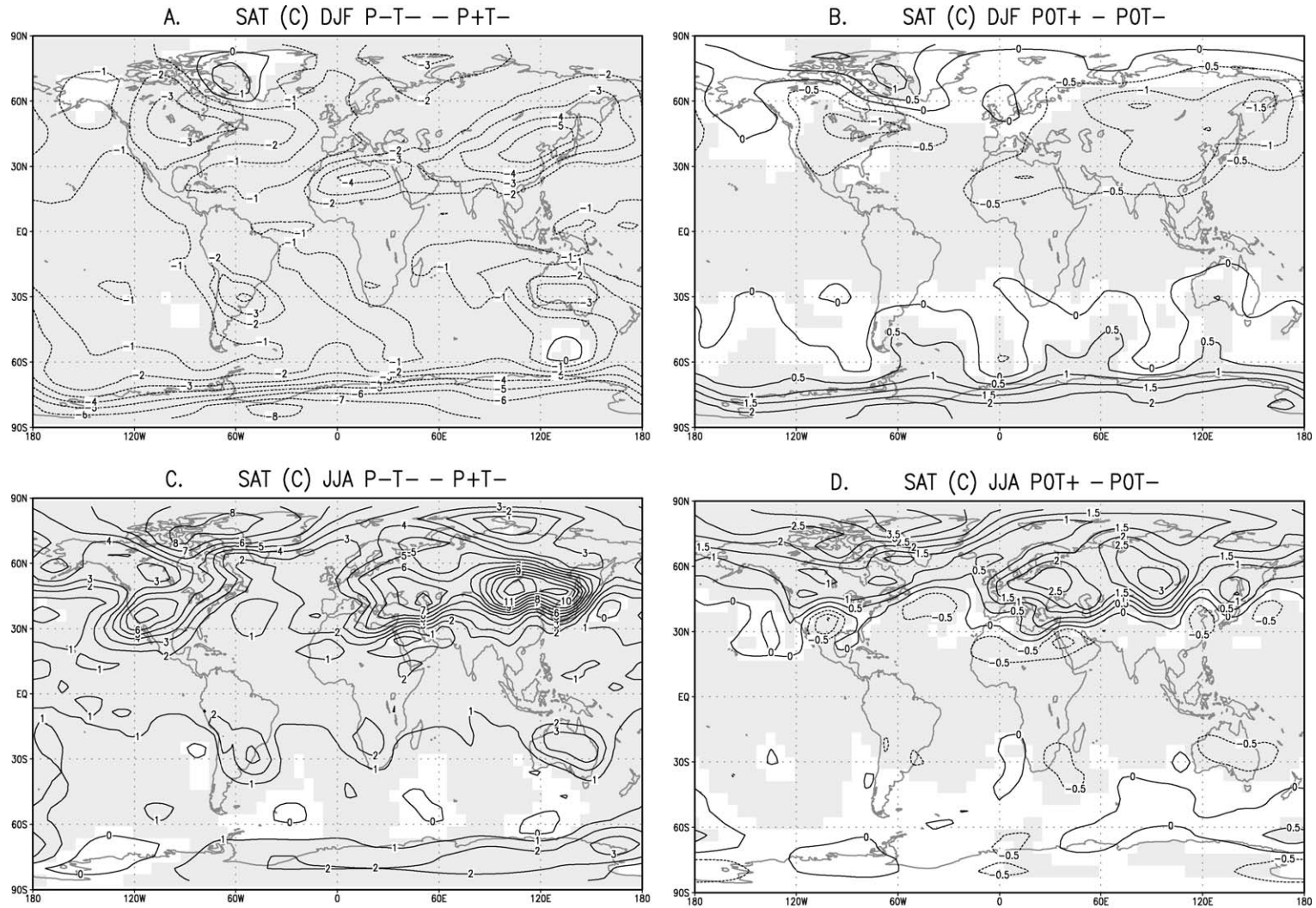


Fig. 2. Seasonal differences of the surface air temperature (SAT) in degrees Celsius. See Table 1 for an explanation of the symbols. (A) December–January–February (DJF) precession signal. (B) Obliquity signal for DJF. (C) June–July–August (JJA) precession signal. (D) Obliquity signal for JJA. Shaded areas are significant at the 99% level, calculated by a local, two-sided Student's t-test. Contour interval is 1°C for (A) and (C), and 0.5°C for (B) and (D).

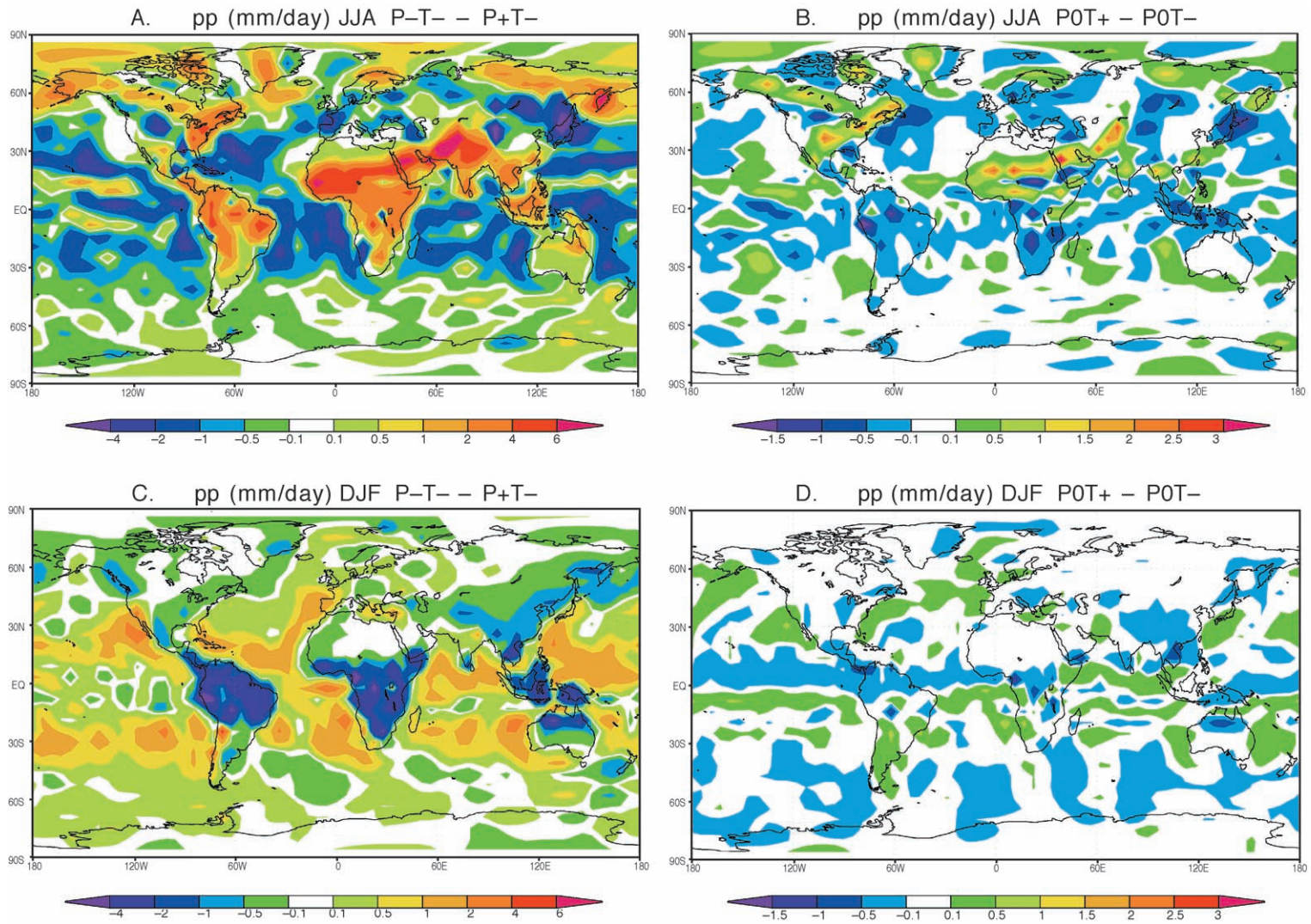


Fig. 3. Same as Fig. 2A–D but now for the precipitation in mm/day. The 99% significance level is approximately at +0.1 and –0.1 mm/day for all figures.

precipitation. The enhanced African monsoon causes the relatively weak or negative signal in the SAT (Fig. 2C and D) because the shortwave radiation is used for enhanced evaporation instead of heating the atmosphere.

In DJF, the precession signal in the precipitation (Fig. 3C) consists of more precipitation over the (subtropical) oceans and less precipitation over the SH monsoon regions during minimum precession. A strong precession signal in the South American monsoon was also found in paleoclimatic data (Martin et al., 1997; Baker et al., 2001). Contrary to precession, obliquity hardly influences the SH monsoons (cf. Fig. 3C and D). Apparently, obliquity-induced insolation differences are too small to influence austral summer monsoonal precipitation.

As with SAT, the obliquity signal in JJA precipitation is different for minimum precession compared to a circular Earth orbit and maximum precession. The response in the African and Asian monsoon is smaller than in the other experiments. This feature will be discussed further in Section 4 where we focus on the African monsoon.

Prell and Kutzbach (1987) used an AGCM to compute the sensitivity of the African and Asian monsoon to changes in the NH insolation in (a perpetual) July. They found a sensitivity of 5 for the African monsoon to obliquity- and precession-induced NH insolation forcing, i.e., a 1% increase in NH solar radiation produces a 5% increase in equatorial North African precipitation. This sensitivity coefficient is comparable to that found in ECBilt.

4. African summer monsoon

The precession-induced zonal mean precipitation differences over North Africa (i.e., zonally averaged over land gridboxes between 10°W and 40°E) show a much stronger maximum during minimum precession compared to maximum precession (i.e., 9 vs. ~6 mm/day, Fig. 4A,B), with a further northward extension of the precipitation during minimum precession. Fig. 4C shows that the precession-induced differences are largest around 20°N and that the largest differences occur 1–2 months after the maximum difference in insolation (Fig. 1A). Comparing precession simulations with a minimum precession, a circular

Earth orbit and a maximum precession (Fig. 4A, E and B, respectively) reveals that the maximum precipitation shifts from July–August, to August and August–September.

In general, obliquity-induced precipitation differences (Fig. 4D,E) show the same pattern as precession. During maximum obliquity, the precipitation extends slightly further northward and its maximum is stronger and located further south with respect to minimum obliquity. The latitudinal displacement of the maximum explains the tripole structure seen in Fig. 3B (see also Fig. 4F). Unlike precession, the obliquity signal does not change the time of occurrence of the maximum precipitation. This also applies to other parameters (e.g., temperature, specific humidity and low-level circulation). The difference pattern (Fig. 4F) shows the largest difference around 20°N and 8°N and it occurs 1–2 months after the maximum difference of the insolation (Fig. 1B).

In order to explain the simulated obliquity and precession signal in the African monsoon, we have examined the specific and relative humidity, surface temperature fields and the large-scale circulation (velocity potential, low-level winds and moisture transport). The vertically averaged specific humidity is larger for minimum precession with the maximum difference north of 20°N (Fig. 5A), while the relative humidity is also increased (Fig. 5C). The increased specific humidity is mainly due to increased temperatures (Fig. 2C) but the increased relative humidity indicates that temperature does not explain the total specific humidity response. The obliquity signal consists of increased specific humidity north of 20°N during maximum obliquity (Fig. 5B), with the temperature either lower or slightly higher over that region (Fig. 2D), resulting in increased relative humidity (Fig. 5D).

Fig. 6A shows the JJA wind vector during minimum precession, together with the difference in wind amplitude between minimum and maximum precession. The precession forcing does not significantly change the direction of the wind. The westerly winds around 15°N over southern north Africa and the tropical Atlantic Ocean are much stronger during minimum precession. This is consistent with an intensified convergence region (centered at 30°N, 80°E; Tibet) and the associated stronger zonal gradient in the velocity potential. The enhanced west-

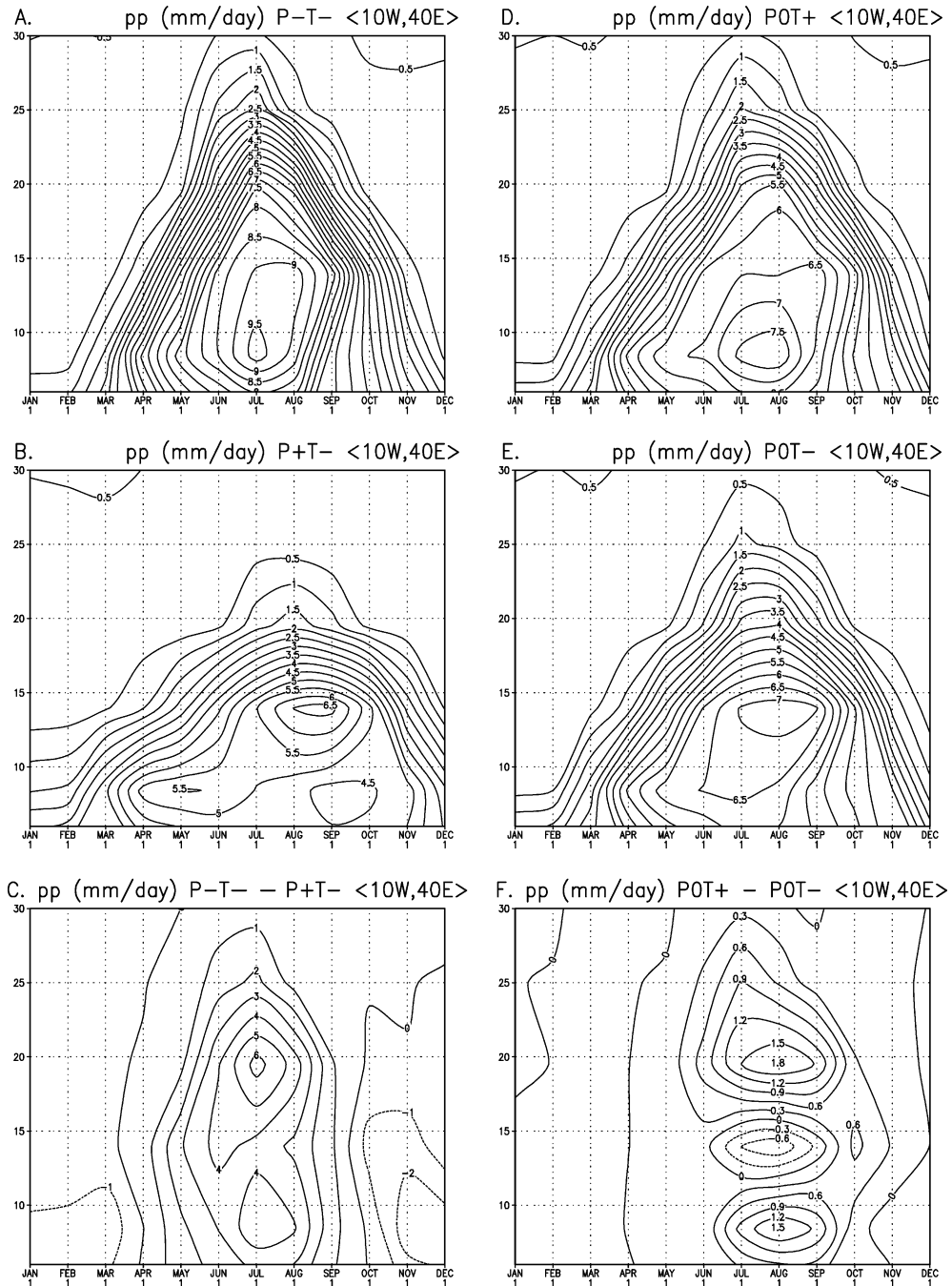


Fig. 4. Zonally averaged ($10^{\circ}\text{W}–40^{\circ}\text{E}$) precipitation (in mm/day) as a function of latitude and month. (A) Minimum precession with minimum obliquity. (B) Maximum precession with minimum obliquity. (C) Difference between (A) and (B), i.e., the response to the precession forcing. (D) Circular Earth orbit with maximum obliquity. (E) Circular Earth orbit with minimum obliquity. (F) Difference between (D) and (E), i.e. the response to the obliquity forcing.

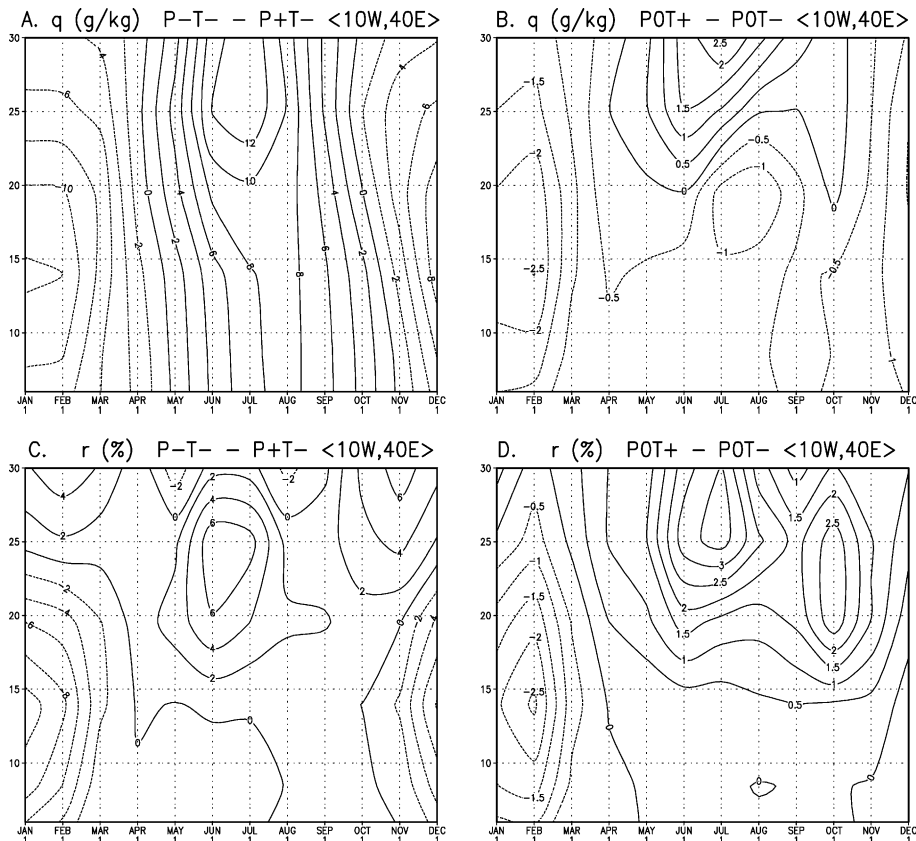


Fig. 5. Same as Fig. 4 but now the response of the specific humidity (g/kg) to (A) the precession forcing and (B) the obliquity forcing. The response of the relative humidity (in %) to (C) the precession forcing and (D) the obliquity forcing.

erlies transport much more moisture to the African continent, which leads to enhanced precipitation. The zonally averaged zonal component of the wind over northwestern Africa ($10^{\circ}\text{W}–15^{\circ}\text{E}$, not shown) reveals that the maximum wind occurs in June/July during minimum precession and in July/August during maximum precession. This is consistent with the timing of the maximum strength of the convergence center over Tibet. Over the Sahara, the northeastern/eastern winds are comparable or even weaker during minimum precession (Fig. 6A). However, the transport of moisture to the south by these weaker winds is still larger due to the large increase in specific humidity (Fig. 5A). Over the Atlantic Ocean the winds associated with the Azores High (AH) are stronger during minimum precession, related to a slightly stronger AH (~ 1 hPa). However, the wind

over the African continent is not strongly influenced by changes in the AH.

The response of the wind to the obliquity signal (Fig. 6B) consists of enhanced westerlies around 15°N during maximum obliquity. Again, the direction of the wind has not significantly changed. Over the northern Sahara, the wind during maximum obliquity is slightly weaker than during minimum obliquity. However, there is still an enhanced transport of moisture into the northern monsoon region due to the increased specific humidity (Fig. 5B). This enhanced moisture transport causes the increased precipitation over the northern monsoon region during maximum obliquity (Fig. 4F). Due to a northward displacement of the AH, the wind is stronger (weaker) over the northern (southern) region of the AH during maximum obliquity (Fig. 6B).

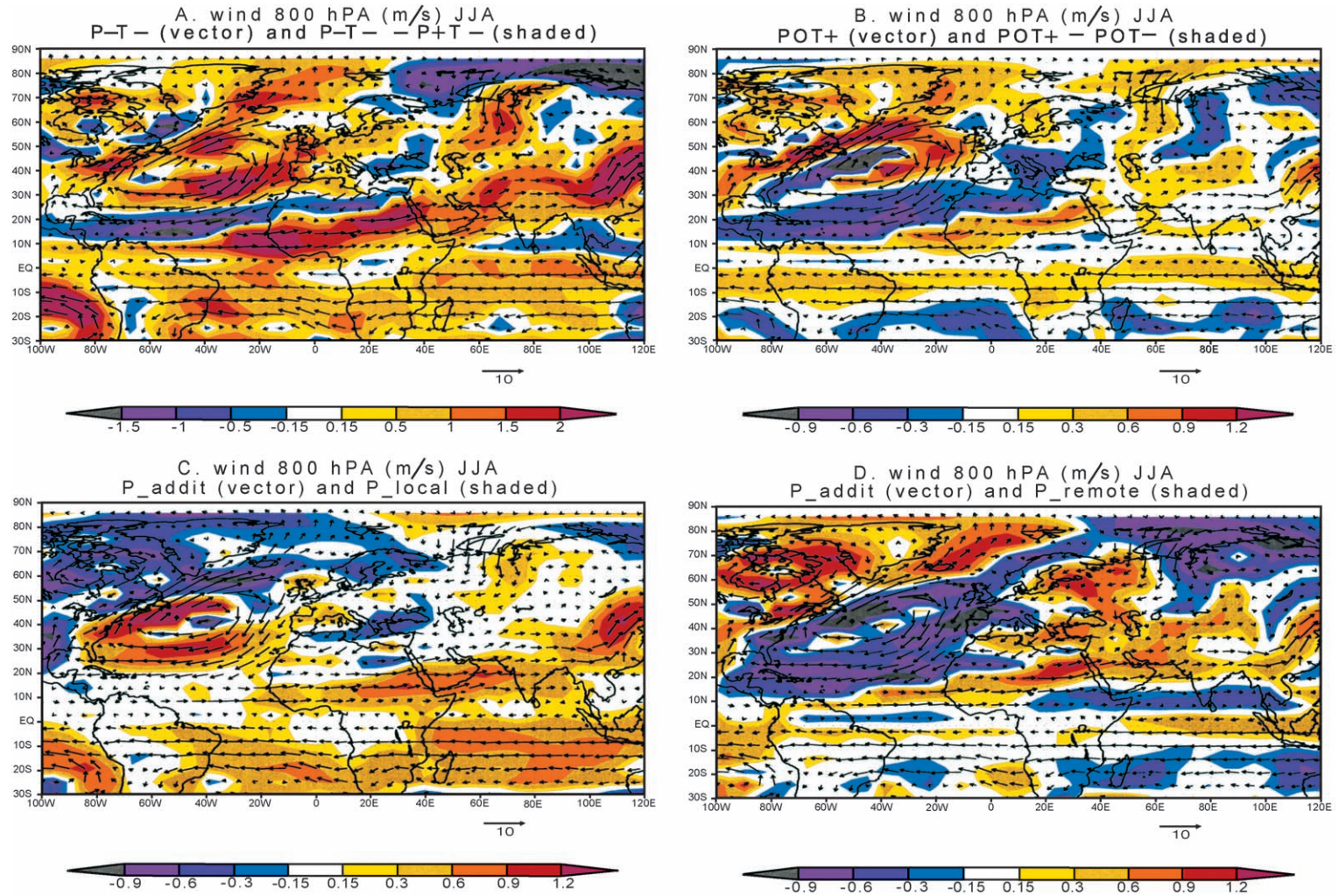


Fig. 6. (A) The wind vector in JJA (m/s) at 800 hPa (arrows) during minimum precession together with the difference (minimum precession minus maximum precession) in wind amplitude (m/s, shaded). (B) Same as (A) but now for maximum obliquity (wind vector; arrows) and the maximum obliquity minus minimum obliquity difference (shaded). (C) Wind vector for the additional precession simulation (see Table 2) and the wind amplitude response to the local precession signal (shaded, see Table 2). (D) Wind vector is similar to (C) together with the wind amplitude response to the remote precession signal (shaded, see Table 2). See also the text for more information. The 99% significance level is approximately at +0.15 and -0.15 m/s for all figures. Note that the scale in (A) differs from (B)–(D).

As noted earlier in Section 3, the obliquity signal with minimum precession differs in some aspects from those with a circular Earth orbit and maximum precession. The obliquity-related JJA precipitation signal over Africa is smaller for a minimum precession than in the other experiments. In particular, around 20°N the differences are about 1.5 to 2 mm/day while south of 20°N the differences are absent. This can be understood as follows. For minimum precession, the obliquity forcing is added to a strong insolation in early summer. This results in low soil moisture in summer and a relatively large signal in SAT. At the same time, the rising branch of the large-scale circulation cell over the African–Asian continent becomes relatively dry and latent heating is reduced. This results in a relatively weak signal in the velocity potential over Asia and a weak response in the zonal wind over northern Africa. Therefore, the precipitation signal is very weak in the southern and central monsoon region. The northern branch is not affected, as the pattern and amplitude of the specific humidity response is similar to that found in the basic experiment. For a circular Earth orbit and maximum precession, the obliquity forcing is added to a smaller insolation. In these cases, the humidity supply for the large-scale circulation is not limited.

5. Local and remote forcing

The obliquity and precession signals in the simulated African summer monsoon give rise to the question whether changes of monsoon intensity are caused by solar radiation changes at high latitudes, at low latitudes, or at a combination of latitudes. In order to examine this issue further, additional simulations have been performed. First we separate the precession signal into a remote effect (i.e., due to the influence of insolation changes north of 30°N) and a local effect (i.e., due to the influence of insolation changes south of 30°N). The local precession signal ‘ P_{local} ’ and the remote precession signal ‘ P_{remote} ’ can be obtained by subtracting an additional experiment ‘ P_{addit} ’ and earlier defined precession experiments, see Table 2. The additional experiment uses an insolation forcing with a minimum precession north of 30°N and a circular Earth orbit south of 30°N, with a maximum obliquity at all latitudes. This set-up does not separate the

Table 2

Orbital configurations used for the additional experiments

P_{addit}	South of 30°N: Circular Earth orbit and maximum obliquity North of 30°N: Minimum precession and maximum obliquity
P_{remote}	Remote precession signal (north of 30°N), i.e. P_{addit} minus P0T+
P_{local}	Local precession signal (south of 30°N), i.e. $P - T+$ minus P_{addit}
$T_{addit30}$	South of 30°N: Circular Earth orbit and minimum obliquity North of 30°N: Circular Earth orbit and maximum obliquity
$T_{addit50}$	South of 50°N: Circular Earth orbit and minimum obliquity North of 50°N: Circular Earth orbit and maximum obliquity
$T_{remote30}$	Remote obliquity signal (north of 30°N), i.e. $T_{addit30}$ minus P0T –
$T_{remote50}$	Remote obliquity signal (north of 50°N), i.e. $T_{addit50}$ minus P0T –

P_{addit} is the additional precession simulation. $T_{addit30}$ and $T_{addit50}$ are additional obliquity simulations.

influence of insolation changes over North Africa (0–30°N) and over the Southern Hemisphere. However, in ECBilt there is a very small transport of air across the equator (see, for example, Fig. 6A) which is mainly due to the quasi-geostrophic approximation. Therefore, in ECBilt insolation changes in the Southern Hemisphere barely influence the African monsoon. The pattern of the insolation forcing for both the remote and the local signal can be derived from Fig. 1A, but the amplitude of the difference is about 50% smaller.

The pattern and amplitude of the precipitation differences induced by the remote forcing (Fig. 7A) is similar to the obliquity-induced differences (Fig. 4F) except that the differences occur 1–2 months earlier. Furthermore, precipitation maxima occur in July during the additional precession simulation and in August during the circular Earth orbit simulation (not shown). The remote influence is most important at subtropical latitudes (20°N–30°N). The largest differences caused by the local precession forcing are located around 15°N (Fig. 7B). The local forcing does not change the timing of the precipitation maxima, which occur both in July (not shown). Comparing the local and remote influence, it can be concluded that the relative importance of each depends strongly

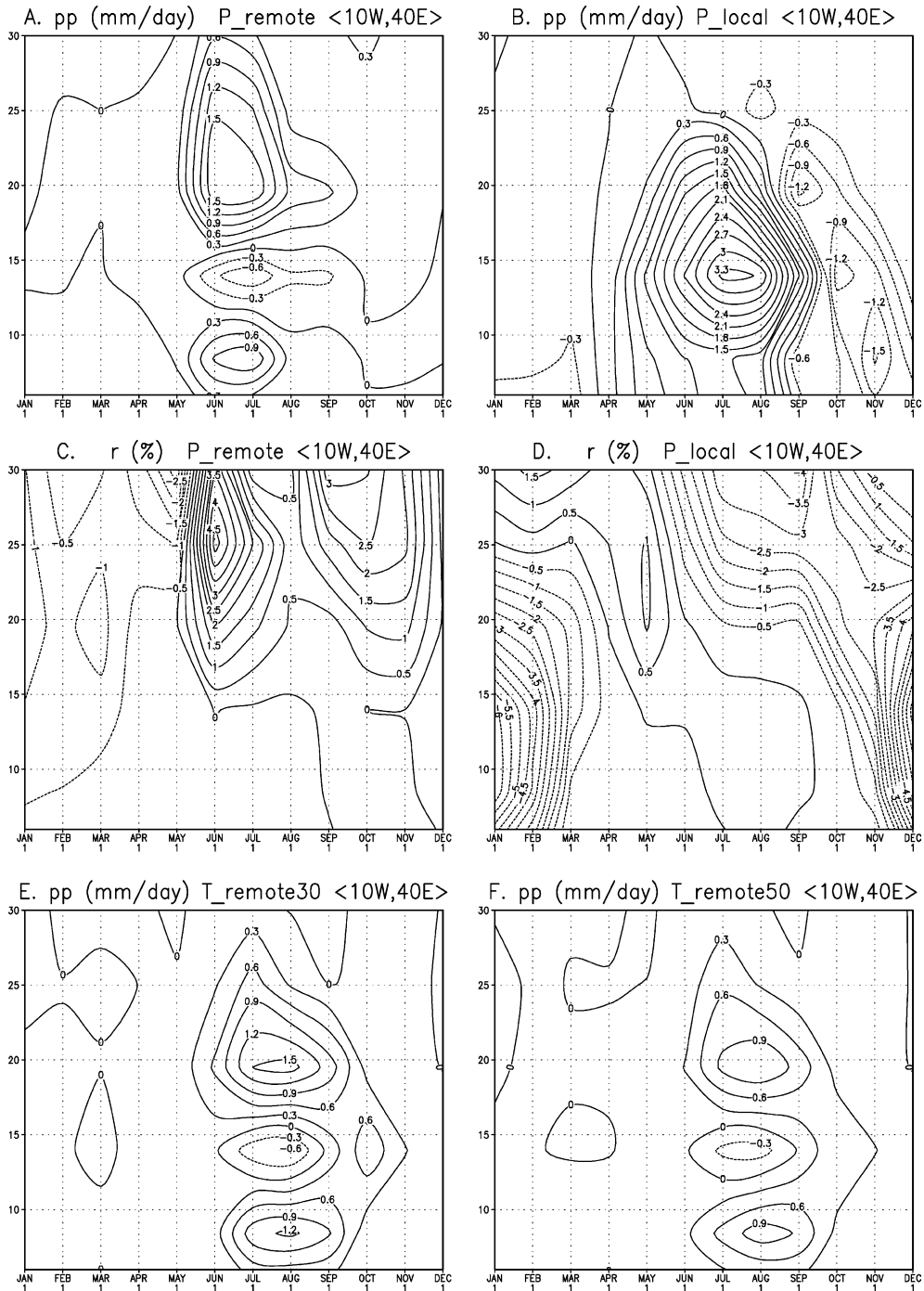


Fig. 7. Same as Fig. 4 but now the response of the precipitation (mm/day) to (A) the remote precession signal and (B) the local precession signal. The response of the relative humidity (in %) to (C) the remote precession signal and (D) the local precession signal. The response of the precipitation (mm/day) to (E) the remote obliquity response (north of 30°N) and (F) the remote obliquity response (north of 30°N). See for more information the text and Table 2.

on latitude. The total difference pattern of the precipitation (i.e., local+remote forcings, not shown) is similar to the pattern shown in Fig. 4C, except that the amplitude is about 50% smaller in agreement with the insolation differences.

The response of the specific humidity to the remote precession signal (not shown) consists of increased specific humidity (~ 4 g/kg) over latitudes around 25°N , similar to the obliquity signal (Fig. 5B). The relative humidity is higher (Fig. 7C), while the temperature is slightly increased (not shown). Examining the vertically averaged moisture transport reveals that the remote signal induces a stronger southward moisture transport into northern Africa resulting in higher specific and relative humidities over northern Africa. The local precession signal in the specific humidity consists of higher values over the entire monsoon region. However, this increase is fully explained by higher temperatures. The relative humidity is even lower (Fig. 7D).

Fig. 6C,D shows that in JJA the enhanced westerlies from the Atlantic Ocean into Africa is a local (Fig. 6C) as well as a remote signal (Fig. 6D). It is not possible to strictly separate the remote and local signal in the large-scale circulation. However, there are some distinctive features. The remotely induced wind response is located further northward and extends into the Asian landmass, while the local signal is restricted to the area south of 30°N . The remote signal is primarily due to the deepening of the large-scale convergence over Asia, while the local signal is a combination of enhanced convergence and the increased heating contrast between the African continent and the adjacent Atlantic Ocean. The zonally averaged zonal wind over northwestern Africa (10°W – 15°E , not shown) shows a temporal shift in the wind maxima in P_{remote} (in June during the additional run and in July during the simulation with the circular Earth orbit) while there is no sign of a shift in P_{local} (both in June). The wind maxima in P_{remote} are concurrent with maxima in the strength of the Asian convergence center. During minimum precession the insolation at high northern latitudes rapidly decreases after its maximum in June, while the maximum precession insolation decreases more slowly (not shown). This results in higher insolation during maximum precession with respect to minimum precession at high latitudes in August–September (Fig. 1A),

causing a shift in the timing of maximum strength of the Asian convergence zone. This, in turn, shifts the timing of the monsoonal circulation and the associated precipitation. Obliquity changes do not change the seasonal pattern of insolation (Fig. 1B) and therefore no obliquity-induced temporal shift in the precipitation is found.

From this additional experiment it follows that the precession signal in precipitation can be separated in a remote and a local signal. The remote precession signal is very similar to the total obliquity signal (cf. Figs. 7A and 4F). The earlier occurrence of the precipitation maximum for minimum precession is found to be a remote signal.

From the results described above it can be concluded that the obliquity signal in the African monsoon originates from insolation changes at mid- to high latitudes. In order to confirm this hypothesis, we performed an additional obliquity simulation, $T_{addit30}$, see Table 2. From this experiment, we obtain the response to the obliquity-induced insolation forcing north of 30°N ($T_{remote30}$, see Table 2). Any effects of the (small amplitude) obliquity forcing at low latitudes are turned off in this additional experiment. The results (Fig. 7E) reveal that the remote forcing north of 30°N accounts for 80–90% of the total signal (cf. Figs. 7E and 4F). To emphasize the role of high latitudes, we repeated this experiment with obliquity forcing restricted to latitudes north of 50°N ($T_{addit50}$ and $T_{remote50}$, see Table 2). The results (Fig. 7F) show that obliquity forcing north of 50°N explains still 60–70% of the total signal (cf. Figs. 7F and 4F). This is partly caused by the insolation-induced increased temperature at high latitudes, resulting in increased specific humidity. This moisture is transported southwards to lower latitudes. A second mechanism for transporting the obliquity signal from high latitudes to lower latitudes is the insolation-induced pressure change at high latitudes. This influences the large-scale circulation and the pressure over central Asia, resulting in a stronger large-scale convergence.

6. Conclusions and discussion

The present study shows that the African summer monsoon is influenced both by obliquity and precession. During either maximum obliquity or minimum

precession the monsoonal precipitation is enhanced and the precipitation extends further northward than during minimum obliquity and maximum precession, respectively. Both the obliquity and the precession signal consist of remote influences (i.e., insolation changes north of 30°N), while the precession signal also consists of a local signal (i.e., insolation changes south of 30°N). The influence of obliquity and the remote influence of precession on African precipitation can be traced back to similar mechanisms. One of the remote mechanisms is stronger wind from the Atlantic Ocean into southern north Africa forced by a deepening of the convergence zone over southern Asia resulting from an increase of summer insolation at high latitudes. Another remote mechanism is penetration of moist air from high latitudes southwards into the northern monsoon region. This is related to the increased ability of the atmosphere to contain water vapour due to the higher temperatures at high latitudes. An additional (local) mechanism of the precession signal is the stronger heating contrast between North Africa and the adjacent Atlantic Ocean which also enhances the low-level monsoonal circulation, bringing relatively moist air to the African continent. Concluding, changes in the monsoon intensity are caused by solar radiation changes at high and at low latitudes.

The time of occurrence of the maximum monsoonal precipitation is influenced by precession but not by obliquity. The insolation maximum shifts through the summer months due to precession, which results in shifts in the maximum strength of the Asian convergence zone and the associated westerlies over northern Africa. Thus, the timing of the precession signal in the African monsoon is primarily a remote effect.

It was found that the precession signal in the African monsoon does not depend on obliquity, while the amplitude of the obliquity signal depends on the prevailing precession. In particular, in the model the obliquity signal is weaker during minimum precession than during maximum precession and a circular Earth orbit. It is a challenge for paleoclimatic studies whether this dependence can also be found in paleoclimatic data, especially for large eccentricity values.

Some important mechanisms for the African summer monsoon are not taken into account in ECBilt. For example, several Holocene studies for 6 ka BP

found that the mutual interaction between vegetation and the atmosphere amplifies the response of the hydrological cycle (Kutzbach et al., 1996; Broström et al., 1998; Ganopolski et al., 1998; Braconnot et al., 1999). Including this mechanism would cause an enhanced sensitivity of the African summer monsoon to obliquity and precession compared to the present results. Another caveat is the use of a simple bucket model, which could cause the dependence of the obliquity signal on the prevailing precession. The very low Asian soil moisture in summer during minimum precession is probably at least in part due to the high sensitivity of the bucket model to temperature changes. Further research with a GCM with a more advanced soil moisture scheme and higher spatial resolution is needed to clarify this point.

The stronger northward extension of the monsoonal precipitation during minimum precession and maximum obliquity consists of only one latitudinal model gridpoint. However, this northward shift has also been found in several generally higher-resolution simulations for 6 ka BP (Braconnot et al., 2002a), and to a stronger extent for 126 ka BP (de Noblet et al., 1996). The orbital-induced northward shift of the African monsoon thus seems to be a realistic feature, which would be enhanced when vegetation is taken into account (e.g., Kutzbach et al., 1996).

Park and Oglesby (1991) performed several runs with an AGCM to study the obliquity and precession influences for the Mid-Cretaceous (100 Ma BP). Although a direct comparison with our results is difficult due to the different geography and topography, some basic features are similar. They noted that the precession signal for most model variables and model regions is stronger than the obliquity signal, even at high latitudes. However, they also found a significant obliquity signal in the hydrological cycle (evaporation minus precipitation) over the equatorial South Atlantic and proto-West Africa (centered around 10°S and 40°W) in a perpetual July. This signal is caused by the circulation changes associated with the impact of obliquity on the southern winter-time pressure maximum.

The results of the present model study are consistent with paleoclimatic data (Pokras and Mix, 1987; Lourens et al., 1996). These studies found a strong precessional component in the strength of the African monsoon. In addition, the obliquity signal found in the

present simulations provides an explanation for the obliquity-related signals in the sedimentary records of the Mediterranean (e.g., Lourens et al., 1996, 2001), through monsoon-induced variations in Nile river outflow and northern Africa aridity.

We have shown that remote forcing (precession and obliquity) and local forcing (precession) both affect the strength of the African summer monsoon. As the phasing of precession does not depend on the latitude, this validates the use of the traditional 65°N Milankovitch insolation curve as a target for tuning sedimentary cycles in the Mediterranean. It is interesting that we find an obliquity signal in the African summer monsoon without the (amplifying) role of glacial ice sheets. This is in agreement with the presence of obliquity signals in the Mediterranean sedimentary records of early Pliocene age (Lourens et al., 1996) and late Miocene age (Hilgen et al., 1995), which are formed well before the onset of the late Pliocene and Pleistocene glacial cycles.

Acknowledgements

This work was supported by the Netherlands Organization for Scientific Research (NWO) under a PIONIER grant to FH. We would like to thank Gerard van der Schrier for helpful discussions and comments on this manuscript.

References

- Baker, P.A., Rigsby, C.A., Seltzer, G.O., Fritz, S.C., Lowenstein, T.K., Bacher, N.P., Veliz, C., 2001. Tropical climate changes at millennial and orbital timescales on the Bolivian Altiplano. *Nature* 409, 698–701.
- Berger, A.L., 1978. Long-term variations of daily insolation and Quaternary climatic changes. *Journal of the Atmospheric Sciences* 35, 2362–2367.
- Braconnot, P., Joussaume, S., Marti, O., de Noblet, N., 1999. Synergistic feedbacks from ocean and vegetation on the African monsoon response to mid-Holocene insolation. *Geophysical Research Letters* 26 (16), 2481–2484.
- Braconnot, P., Loutre, M.-F., Dong, B., Joussaume, S., Valdes, P., PMIP Participating Groups, 2002a. How the simulated change in monsoon at 6 ka BP is related to the simulation of the modern climate: results from the Paleoclimate Modeling Intercomparison Project. *Climate Dynamics* 19, 107–121.
- Braconnot, P., Harrison, S., Hewitt, C.D., Kitoh, A., Otto-Bliesner, B., Weber, S.L., 2002b. Results of the PMIP working group on coupled ocean–atmosphere simulations for 6 ka BP. To appear in ‘Past Climate Variability Through Europe and Africa’. Proceedings of the PAGES-PEP3 Conference, 27–31 August 2001, Aix-en-Provence, France.
- Broström, A., Coe, M., Harrison, S.P., Gallimore, R., Kutzbach, J.E., Foley, J., Prentice, I.C., Behling, P., 1998. Land surface feedbacks and palaeomonsoons in northern Africa. *Geophysical Research Letters* 25 (19), 3615–3618.
- de Noblet, N., Braconnot, P., Joussaume, S., Masson, V., 1996. Sensitivity of simulated Asian and African summer monsoons to orbitally induced variations in insolation 126, 115 and 6 kBP. *Climate Dynamics* 12, 589–603.
- Ganopolski, A., Kubatzki, C., Claussen, M., Brovkin, V., Petoukhov, V., 1998. The influence of vegetation–atmosphere–ocean interaction on climate during the mid-Holocene. *Science* 280, 1916–1919.
- Harvey, L.D.D., 1989. Milankovitch forcing, vegetation feedback, and North Atlantic deep-water formation. *Journal of Climate* 2, 800–815.
- Hilgen, F.J., 1991. Astronomical calibration of Gauss to Matuyama sapropels in the Mediterranean and implication for the geomagnetic polarity time scale. *Earth and Planetary Science Letters* 104, 226–244.
- Hilgen, F.J., Krijgsman, W., Langereis, C.G., Lourens, L.J., Santarelli, A., Zachariasse, W.J., 1995. Extending the astronomical (polarity) time scale into the Miocene. *Earth and Planetary Science Letters* 136 (3), 495–510.
- Joussaume, S., Taylor, K.E., Braconnot, P., Mitchell, J.F.B., Kutzbach, J.E., Harrison, S.P., Prentice, I.C., Broccoli, A.J., Abe-Ouchi, A., Bartlein, P.J., Bonfils, C., Dong, B., Guiot, J., Herterich, K., Hewitt, C.D., Jolly, D., Kim, J.W., Kislov, A., Kitoh, A., Loutre, M.F., Masson, V., McAveny, B., McFarlane, N., de Noblet, N., Peltier, W.R., Peterschmitt, J.Y., Pollard, D., Rind, D., Royer, J.F., Schlesinger, M.E., Syktus, J., Thompson, S., Valdes, P., Vettoretti, G., Webb, R.S., Wyputta, U., 1999. Monsoon changes for 6000 years ago: results of 18 simulations from the Paleoclimate Modeling Intercomparison Project (PMIP). *Geophysical Research Letters* 26 (7), 859–862.
- Kistler, R., Kalnay, E., Collins, W., Saha, S., White, G., Woollen, J., Chelliah, M., Ebisuzaki, W., Kanamitsu, M., Kousky, V., van den Dool, H., Jenne, R., Fiorino, M., 2001. The NCEP-NCAR 50-year reanalysis: monthly means CD-ROM and documentation. *Bulletin of the American Meteorological Society* 82 (2), 247–267.
- Kutzbach, J.E., 1981. Monsoon climate of the early Holocene: climate experiment with the Earth’s orbital parameters for 9000 years ago. *Science* 214, 59–61.
- Kutzbach, J.E., Otto-Bliesner, B.L., 1982. The sensitivity of the African–Asian monsoonal climate to orbital parameter changes for 9000 years B.P. in a low-resolution general circulation model. *Journal of the Atmospheric Sciences* 39 (6), 1177–1188.
- Kutzbach, J.E., Street-Perrott, F.A., 1985. Milankovitch forcing of fluctuations in the level of tropical lakes from 18 to 0 kyr BP. *Nature* 317, 130–134.
- Kutzbach, J., Bonan, G., Foley, J., Harrison, S.P., 1996. Vegetation and soil feedbacks on the response of the African monsoon to

- orbital forcing in the early to middle Holocene. *Nature* 384, 623–626.
- Lourens, L.J., Antonarakou, A., Hilgen, F.J., Van Hoof, A.A.M., Vergnaud-Grazzini, C., Zachariasse, W.J., 1996. Evaluation of the Plio-Pleistocene astronomical timescale. *Paleoceanography* 11 (4), 391–413.
- Lourens, L.J., Wehausen, R., Brumsack, H.J., 2001. Geological constraints on tidal dissipation and dynamical ellipticity of the Earth over the past three million years. *Nature* 409, 1029–1033.
- Martin, L., Bertaux, J., Corrège, T., Ledru, M.-P., Mourguiart, P., Sifeddine, A., Soubiès, F., Wirmann, D., Suguio, K., Turcq, B., 1997. Astronomical forcing of contrasting rainfall changes in tropical South America between 12,400 and 8800 cal yr B.P. *Quaternary Research* 47, 117–122.
- Opsteegh, J.D., Haarsma, R.J., Selten, F.M., Kattenberg, A., 1998. ECBILT: a dynamic alternative to mixed boundary conditions in ocean models. *Tellus* 50A, 348–367.
- Park, J., Oglesby, R.J., 1991. Milankovitch rhythms in the Cretaceous: a GCM modelling study. *Palaeogeography, Palaeoclimatology, Palaeoecology* 90, 329–355.
- Pokras, E.M., Mix, A.C., 1987. Earth's precession cycle and Quaternary climatic change in tropical Africa. *Nature* 326, 486–487.
- Prell, W.L., 1984. Monsoonal climate of the Arabian Sea during the late Quaternary: a response to changing solar radiation. In: Berger, A.L., et al. (Eds.), *Milankovitch and Climate*, vol. 1. Reidel, Dordrecht, pp. 349–366.
- Prell, W.L., Kutzbach, J.E., 1987. Monsoon variability over the past 150,000 years. *Journal of Geophysical Research* 92 (D7), 8411–8425.
- Rosignol-Strick, M., 1983. African monsoons, an immediate climate response to orbital insolation. *Nature* 304, 46–49.
- Short, D.A., Mengel, J.G., Crowley, T.J., Hyde, W.T., North, G.R., 1991. Filtering of Milankovitch cycles by Earth's geography. *Quaternary Research* 35, 157–173.
- Suarez, M.J., Held, I.M., 1979. The sensitivity of an energy balance climate model to variations in the orbital parameters. *Journal of Geophysical Research* 84 (C8), 4825–4836.
- Van der Schrier, G., Weber, S.L., Drijfhout, S.S., 2002. Sea level changes in the North Atlantic by solar forcing and internal variability. *Climate Dynamics* 19, 435–447.
- Weber, S.L., 2001. The impact of orbital forcing on the climate of an intermediate–complexity coupled model. *Global and Planetary Change* 30, 7–12.
- Weber, S.L., Oerlemans, J., 2003. Holocene glacier variability: three case studies using an intermediate–complexity model. *The Holocene* (in press).